

IRENE SHIVAEI<sup>1,7</sup>, MARISKA KRIEK<sup>2</sup>, NAVEEN A. REDDY<sup>1</sup>, ALICE E. SHAPLEY<sup>3</sup>, GUILLERMO BARRO<sup>2</sup>, CHARLIE CONROY<sup>4</sup>, ALISON L. COIL<sup>5</sup>, WILLIAM R. FREEMAN<sup>1</sup>, BAHRAM MOBASHER<sup>1</sup>, BRIAN SIANA<sup>1</sup>, RYAN SANDERS<sup>3</sup>, SEDONA H. PRICE<sup>2</sup>, MOJEGAN AZADI<sup>5</sup>, IMAD PASHA<sup>2</sup>, HANA E. INAMI<sup>6</sup>

ACCEPTED TO APJL: March 5, 2016

ABSTRACT

We present the first direct comparison between Balmer line and panchromatic SED-based SFRs for  $z \sim 2$  galaxies. For this comparison we used 17 star-forming galaxies selected from the MOSFIRE Deep Evolution Field (MOSDEF) survey, with  $3\sigma$  detections for  $H\alpha$  and at least two IR bands (*Spitzer*/MIPS 24  $\mu\text{m}$  and *Herschel*/PACS 100 and 160  $\mu\text{m}$ , and in some cases *Herschel*/SPIRE 250, 350, and 500  $\mu\text{m}$ ). The galaxies have total IR (8 – 1000  $\mu\text{m}$ ) luminosities of  $\sim 10^{11.4} - 10^{12.4} L_{\odot}$  and star-formation rates (SFRs) of  $\sim 30 - 250 M_{\odot} \text{yr}^{-1}$ . We fit the UV-to-far-IR SEDs with flexible stellar population synthesis (FSPS) models – which include both stellar and dust emission – and compare the inferred SFRs with the SFR( $H\alpha, H\beta$ ) values corrected for dust attenuation using Balmer decrements. The two SFRs agree with a scatter of 0.17 dex. Our results imply that the Balmer decrement accurately predicts the obscuration of the nebular lines and can be used to robustly calculate SFRs for star-forming galaxies at  $z \sim 2$  with SFRs up to  $\sim 200 M_{\odot} \text{yr}^{-1}$ . We also use our data to assess SFR indicators based on modeling the UV-to-mid-IR SEDs or by adding SFR(UV) and SFR(IR), for which the latter is based on the mid-IR only or on the full IR SED. All these SFRs show a poorer agreement with SFR( $H\alpha, H\beta$ ) and in some cases large systematic biases are observed. Finally, we show that the SFR and dust attenuation derived from the UV-to-near-IR SED alone are unbiased when assuming a delayed exponentially declining star-formation history.

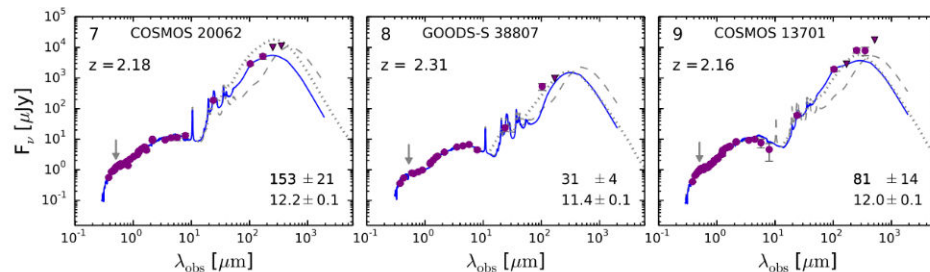


Figure 2. The best-fit panchromatic FSPS SED models (solid curves) to the observed photometry (purple symbols) of 9 of our  $H\alpha+H\beta$ -detected galaxies. The rest-frame optical emission lines are excluded from both the photometry and the models. The triangles show  $3\sigma$  upper limits on the fluxes; in the fitting process, the actual photometry with the corresponding errors were used. The dashed and dotted lines represent the FSPS SED fits up to 24  $\mu\text{m}$  and the Chary & Elbaz (2001) best-fit templates to the 24, 100, and 160  $\mu\text{m}$  data, respectively. The ID numbers are from the 3DHST v4.1 photometric catalog. The galaxies are shown in order of increasing mass (continued in Figure 3).

UV-FIR full SED-fittingの例

SFRの比較

SFR( $H\alpha$ ) vs. SFR(UV-FIR SED) @  $z \sim 2$

- ❑ MOSDEF data:  $H\alpha$ ,  $H\beta$  (if detected)
- ❑ CANDELS multi- $\lambda$  data: UV~Opt, IRAC, MIPS 24 $\mu\text{m}$ , PACS 100/160 $\mu\text{m}$ , SPIRE 250/350/500 $\mu\text{m}$
- ❑ Sample selection: 13 (with  $H\beta$ ), 4 (without  $H\beta$ )
  - ❑  $H\alpha$  (S/N>3), 24 $\mu\text{m}$  (S/N>3), 100 or 160 $\mu\text{m}$  detected
- ❑ UV-FIR SED fitting (Flexible Stellar Population Synthesis)
  - ❑ Dustによる「UV光吸収」と「FIR再放射」のenergy balance
  - ❑ Delayed tau star-formation history

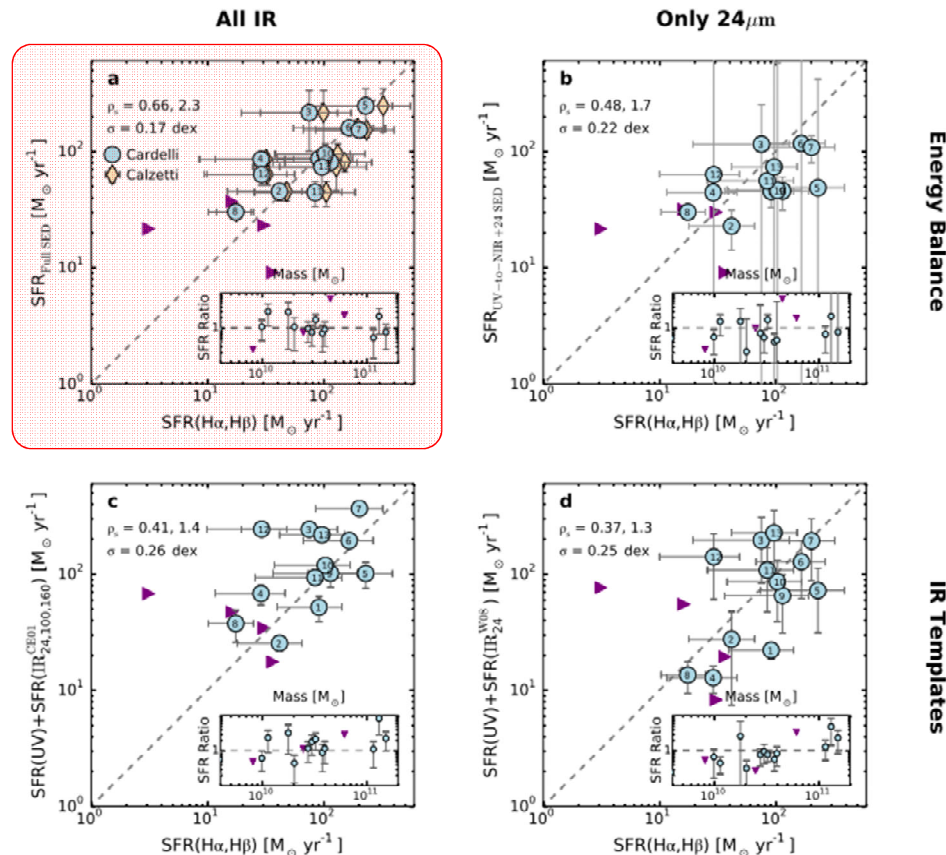
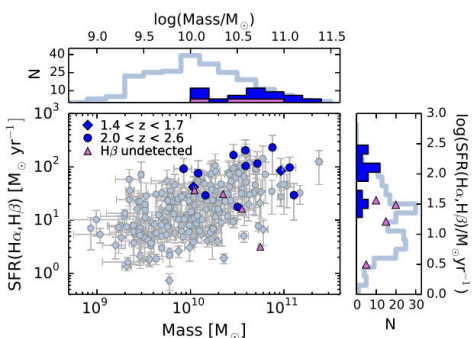


Figure 4. SFR comparisons for the 13  $H\alpha+H\beta$ -detected galaxies (circles) and the 4  $H\beta$ -undetected galaxies (triangles). In all plots, the horizontal axis is the SFR( $H\alpha, H\beta$ ), assuming the Cardelli curve, and the dashed lines denote one-to-one relationships. In panel a, diamonds indicate SFR( $H\alpha, H\beta$ ) assuming the Calzetti curve. The vertical axis is the SFR derived from modeling the UV-to-FIR photometry (a), the UV-to-24  $\mu\text{m}$  photometry (b), and SFR(UV)+SFR(IR), in which SFR(IR) is derived from 24 – 160  $\mu\text{m}$  (c) or 24  $\mu\text{m}$  only photometry (d), using the CE01 and W08 templates, respectively. Each subplot shows the ratio of the SFR in the main plot's vertical axis to SFR( $H\alpha, H\beta$ ) as a function of  $M_*$ . The masses are inferred from the best-fit SEDs. The Spearman coefficient ( $\rho_s$ ), its significance, and scatter about the unity line ( $\sigma$ ) are listed in the plots. The galaxies' numbers correspond to the SEDs in Figures 2,3.

Balmer decrementで減光補正したSFR( $H\alpha$ )は、UV-FIRのfull SED fittingから推定されるSFR(full SED)と $\sim 0.2$  dexで一致した。



今後詰めるべきSFRの不定性:

- extinction curve, IMF, metallicity, SFH
  - dust emission model
- MOSDEF/PACS/SPIRE sampleが増えればstackingで見てみる。

MOSDEF全サンプルと今回の17天体のMs-SFR上での分布